01 Jan 2005

Measurement and Prediction of Pressure Drop in Pneumatic Conveying: Effect of Particle Characteristics, Mass Loading, and Reynolds Number

Kimberly H. Henthorn
Missouri University of Science and Technology

Kinam Park

Jennifer S. Curtis

f-electron correlations in nonmagnetic Ce studied by means of spin-resolved resonant photoemission

S.-W. Yu,[1,*] T. Komesu,[2] B. W. Chung,[1] G. D Waddill,[2] S. A. Morton,[1,2] and J. G. Tobin[1]
[1]*Lawrence Livermore National Laboratory, Livermore, California 94550, USA*
[2]*Physics Department, University of Missouri-Rolla, Rolla, Missouri 65409, USA*
(Received 14 October 2005; published 23 February 2006)

We have studied the spin-spin coupling between two *f* electrons of nonmagnetic Ce by means of spin-resolved resonant photoemission using circularly polarized synchrotron radiation. The two *f* electrons participating in the $3d_{5/2} \rightarrow 4f$ resonance process are coupled in a singlet while the coupling is veiled in the $3d_{3/2} \rightarrow 4f$ process due to an additional Coster-Kronig decay channel. The identical singlet coupling is observed in the $4d \rightarrow 4f$ resonance process. Based on the Ce measurements, it is argued that spin-resolved resonant photoemission is one approach to study the correlation effects, particularly in the form of spin, in the rare earths.

DOI: 10.1103/PhysRevB.73.075116 PACS number(s): 71.28.+d, 72.25.Fe, 79.60.−i

In photoemission investigations of nonmagnetic materials, the measurement of electron spin polarization, with respect to a suitably chosen quantization direction, can provide insight into the electronic structure of the systems under study, beyond that which can be gleaned from merely the energy and momentum relationship of the photoelectrons.[1,2] For example, the spin-polarized photoemission experiment performed with circularly polarized light, in which spin polarization is aligned with photon propagation direction, is an essential method to characterize the symmetries of the states. These measurements permit the performance of the symmetry resolved band mapping of solids[3–6] and the determination of all dipole matrix elements and phase-shift differences of continuum wave functions describing the photoelectron emission from free and absorbed atoms.[6] The combination of a spin-orbit interaction and circularly polarized light induces an anisotropic distribution of the m_j in the final state wave function via the relativistic dipole selection rules. To a great extent, these measurements are extensions of the Fano effect, predicted[7] and observed[8] over 30 years ago.

The photoexcitation of core electrons by circularly polarized light in nonmagnetic materials will not only result in the spin polarization of the ejected photoelectrons[9] but also in spin-polarized core holes aligned with photon spin. These spin-polarized core holes can decay by emission of polarized photons or by spin dependent Auger processes.[10–18] For example, consider the CVV (core valence valence) Auger process in a solid. The initial state is two valence electrons and the final state is two electron states in which one of them has filled the polarized hole and another one is ejected as an Auger electron. If the two valence electrons are coupled in a singlet, the spin of the outgoing electron has to be antiparallel to the spin of the primary core hole, due to the selection rules governing the Auger process ($\Delta S=0$).[19] If the two valence electrons are coupled in a triplet, the spin of the outgoing electron has to be parallel to the spin of the primary core hole. Therefore, the spin analysis of the photoelectrons and the corresponding Auger electrons allows the study of the spin-spin coupling between the two valence electrons participating in the CVV decay process from the nonmagnetic materials.

In the above context, this paper reports on the spin-resolved measurements of the $3d \rightarrow 4f$ resonant photoemission in nonmagnetic Ce, as a means of studying electron correlations between *f* electrons. Furthermore, because Ce is the first element of the rare earths and the location of the delocalized/localized transition in the rare earths,[20] the results from Ce may serve as a prototype for the other rare earths, in which strong correlation effects originating from highly localized *f* electrons may play a crucial role for the determination of the physical properties.[21–24] Here, it will be shown that spin-resolved resonant photoemission spectroscopy, using circularly polarized light, can provide a direct means of investigating electron correlation in nonmagnetic materials. In this case, it will be shown that electron-electron coupling in the Auger-like decay process can be observed in a powerful manner.

The experiments were performed at the beamline 4-ID-C of the Advanced Photon Source, at Argonne National Laboratory.[25] The beamline provides circularly polarized x rays, with switchable helicities ($\sigma^{\pm}$) on demand, with a degree of polarization >96% in the energy range of 500–3000 eV. The total resolution (beamline+analyzer) of 0.8 eV was chosen to allow a reasonable signal in the Mott detector, since the efficiency of the Mott detector ($S^2 I/I_0$) is of the order 10^{-5}. The experimental apparatus used in the present study has been previously described.[26–28] Uncrystallized cerium samples were made by evaporation *in situ* on a W(110) substrate at room temperature.[29] Our samples are close to the γ-Ce.[20] The base pressures were in the low 10^{-11} torr range, rising to $\sim 6 \times 10^{-10}$ torr during evaporation. The cleanliness of the Ce samples was monitored by an O 1*s* signal. In order to make sure the samples are free from oxygen, fresh samples were made approximately every 6 h, and cleanliness was controlled before and after the measurements. No oxygen contaminations were indicated in the samples. Photon energies were calibrated using the $3d_{5/2} \rightarrow 4f$ transition in x-ray absorption spectroscopy (XAS), at an energy of 882.2 eV (Ref. 30.)

For our purposes the $3d \rightarrow 4f$ transition of Ce is an excellent choice because the spin-orbit split $3d_{5/2}$ and $3d_{3/2}$ levels are well separated by 18.5 eV in binding energy.[21] Thus well

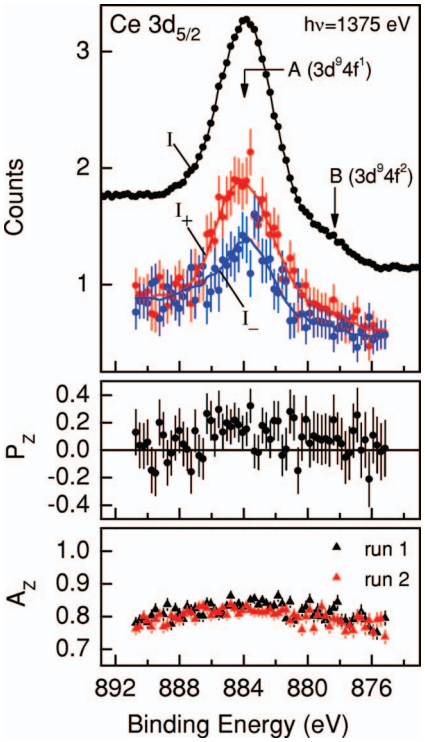

FIG. 1. (Color) Top panel; spin resolved $3d_{5/2}$ photoemission spectrum of Ce generated with circularly polarized light of $h\nu = 1375$ eV. I is the spin integrated total intensity, and I_+ (red) and I_- (blue) are the two spin separated partial intensities. The solid lines on I_+ and I_- serve as a guide to the eyes. Middle panel; electron spin polarization P_Z aligned with photon propagation direction determined by Eq. (3). The vertical error bars given in P_Z represent the single statistic uncertainties in the measured spin polarization. Bottom panel; instrumental asymmetries A_Z determined by Eq. (4) for the two independent runs.

defined and oppositely spin-polarized core holes can potentially be generated by photoexcitation using circularly polarized light into the $4f$ final states. The $3d \rightarrow 4f$ resonance arises when an interference occurs between the direct photoemission channel,

$$3d^{10}4f^1 + h\nu \rightarrow 3d^{10}4f^0 + \text{electron}, \tag{1}$$

and an indirect channel in which there is the $3d \rightarrow 4f$ excitation with subsequent CVV Auger-like decay,

$$3d^{10}4f^1 + h\nu \rightarrow 3d^9 4f^2 \rightarrow 3d^{10}4f^0 + \text{electron}, \tag{2}$$

which has the identical initial and final state with the direct channel. Since the condition for the interference is coherence between the direct and the indirect channels, the loss of coherence can be due either to delocalization of the $4f$ electrons in the intermediate state, which produces an energy difference between the final states of the two channels or to a different time for the two channels.[31,32] Therefore, the sharp resonance in the $3d \rightarrow 4f$ transition is consistent with the strongly localized nature of $4f$ wave functions in rare earths.[30]

A spin-resolved core level spectrum is shown in Fig. 1. Here, the Ce $3d_{5/2}$ level at a binding energy of 883.8 eV is undergoing interrogation with photons of 1375 eV. With photons of 1375 eV, $3d$ direct photoelectrons have a kinetic energy of ~500 eV, which is good energy for an optimum operation of the Mott detector, and are well separated from the $3p$ direct photoemission peaks and *MNN* Auger peaks, and any peaks associated with $3p$ core holes. The $3d_{5/2}$ level will be one of those used in the resonant photoemission study. Measurements of its spin polarization is essential to establishing the initial polarizations of the core holes and testing the validity of our relativistic models. In order to eliminate the instrumental asymmetry, the electron spin polarization P_Z aligned to the photon spin is determined from the raw spectra using the following formula:

$$P_Z = \frac{1}{SP_\sigma \cos 55} \left(\frac{\sqrt{N_1^+ N_3^-} - \sqrt{N_1^- N_3^+}}{\sqrt{N_1^+ N_3^-} + \sqrt{N_1^- N_3^+}} \right). \tag{3}$$

Here, $N^{\pm}_{1(3)}$ is the intensity with $\sigma^{\pm}$ at the counters 1(3) located at equal polar angles 120° in the reaction plane defined by the incoming and scattered electron beam, P_σ is the light polarization, and cos 55° is due to the 55° off-normal incidence of light and the normal emission of electrons. The Sherman function S, which describes the sensitivity of the Mott detector, is 0.12 (Ref. 26). It should be noted that the instrumental asymmetry A_Z defined in the following way:

$$A_Z = \frac{\sqrt{N_1^+ N_1^-}}{\sqrt{N_3^+ N_3^-}}, \tag{4}$$

has to be monitored for every run to determine the electron spin polarization correctly.[33] If A_Z differs from 1, this means that there is an instrumental asymmetry. The instrumental asymmetry can be eliminated by using Eq. (3) only if A_Z does not vary in time.[33] Therefore, the monitoring of A_Z provides an important check on the performance of the Mott detector. If A_Z is not constant over runs, the spin polarization determined by using Eq. (3) cannot be claimed to be accurate. For example, the bottom panel of Fig. 1 shows that we have an instrumental asymmetry because A_Z differs from 1, and that the instrumental asymmetry can be eliminated by using Eq. (3) because A_Z is constant over runs. The middle panel of Fig. 1 shows the P_Z measured by using Eq. (3).

In the top of Fig. 1, the spin-separated partial intensities I_+ and I_- are connected with the measured spin polarization P_Z and the measured total (spin-independent) intensity I by $I_\pm = I/2(1 \pm P_Z)$. Correspondingly, I_+ and I_- are the partial intensities polarized totally parallel and antiparallel to the photon spin, respectively. From the total intensity I, a strong main peak A centered at a binding energy of 883.8 eV and a weak peak B centered at a binding energy of ~878 eV are visible. The physical origin of the two peaks can be understood in terms of the configuration interaction as follows. Because $4f$ states are localized in the $3d$ core region, they are extremely sensitive to the attractive Coulomb potential of the $3d$ hole.

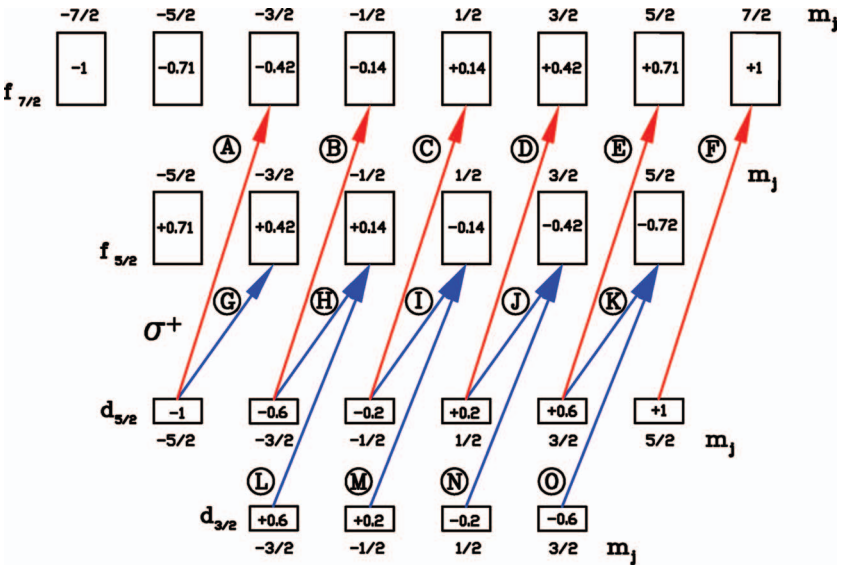

FIG. 2. (Color) Scheme of the photoexcitation $d \rightarrow f$ with σ^+. The arrows indicate the allowed transitions via relativistic dipole selection rules for σ^+ with the following transition probabilities normalized to transition G. $A=5/2$, $B=15/2$, $C=30/2$, $D=50/2$, $E=75/2$, $F=105/2$, $G=1$, $H=8/5$, $I=9/5$, $J=8/5$, $K=1$, $L=49/10$, $M=147/10$, $N=147/5$, $O=49$. Thereby, identical radial parts of the $d_{5/2}$ and $d_{3/2}$ wave functions and of the $f_{7/2}$ and $f_{5/2}$ wave functions are assumed. The arrows with red (blue) color represent the transitions which give a positive (negative) spin polarization of the photoelectrons. The $d_{5/2} \rightarrow f_{5/2}$ transition gives a negative spin polarization, but it has 20 times weaker transition probability than that of the $d_{5/2} \rightarrow f_{7/2}$. Therefore, $d_{5/2} \rightarrow f$ $(f_{7/2}+f_{5/2})$ transition gives a net positive spin polarization of the photoelectrons. Positive and negative numbers in the rectangles give the angle integrated spin polarization for given m_j using the Clebsch-Gordan coefficients, e.g., for $m_j=-3/2$ of $d_{5/2}$, $|d_{5/2}, m_j=-3/2\rangle = \sqrt{1/5}Y_{2,-2}|\uparrow\rangle + \sqrt{4/5}Y_{2,-1}|\downarrow\rangle$ (Ref. 10), therefore, −0.6 spin polarization. The energy differences are not to scale.

Consequently, the creation of a $3d$ core hole by photoexcitation causes an additional empty $4f$ state to be pulled down below the Fermi energy. Thus, in a very simple picture, two final states are produced; when the empty $4f$ state is not yet occupied and the screening is produced by the $(5d6s)^3$ valence band, the result is a final state with a configuration of $3d^9 4f^1$ (peak A). If the empty $4f$ state is filled by an extra f electron from the conduction band and it screens the core hole, this is another final state with a configuration of $3d^9 4f^2$ (peak B). The second final state with the configuration of $3d^9 4f^2$ has a much weaker intensity and smaller binding energy.[21,34–37] From the spin separated partial intensities I_+ and I_-, it can be seen that I_+ is dominant over peak A, with an approximately +20% spin polarization. It is interesting to note that peak B is also slightly positively polarized.

For convenience, the configuration interaction model has been used to explain the double $3d_{5/2}$ structures of Ce in this paper. But, it should be noted that there is another description for strongly correlated electron systems using a modified Anderson impurity model,[38–40] which describes the features of the valence band spectra and of the core-level spectra as well.

We use the three-step model of photoemission in the interpretation of the spin-resolved spectra. It should be noted that even though the three-step model explains the experimental data for the bulk photoemission surprisingly well, there is a conceptual deficiency. The disadvantages of the three-step model are overcome by the one-step model of photoemission, in which the photoemission process is considered as a one-step quantum mechanical event.[41–43] However, in our case, the dominant effect is the spin-dependent optical pumping process induced by the circularly polarized x-rays, which can be dealt with most easily in the first step of the three-step model. The three-step model consists of (i) the primary excitation process in the bulk by absorption of the incident photon, (ii) the transport of the excited electron to the surface which includes the possibility for inelastic scattering by the electron-electron and the electron-phonon, and (iii) the escape of the electron through the surface into the vacuum.[44] In principle, every one of these three steps may result in a nonzero contribution to the net spin polarization. For centrosymmetric nonmagnetic materials with no preferential population of one spin state in the ground state, however, it is demonstrated that the first step, the primary excitation process, is mainly responsible for nonzero spin polarization if the exciting light is circularly polarized.[2] The second step, transport to the surface, produces no net spin polarization in nonmagnetic materials.[2] In the third step, off-normally emitted photoelectrons may require a nonzero contribution to the net spin polarization during their transmission through the surface due to the spin-dependent diffraction of the photoelectrons at the surface.[45–47] However, this contribution to the net spin polarization vanishes for the symmetry reasons for normal emission to the surface.[45] Therefore, nonmagnetic materials and normal emission of electrons ensure that the second and the third step of the three-step model of photoemission are spin-independent, and the spin polarization is dominated by the primary excitation known as optical spin orientation.[1,2] Fig-

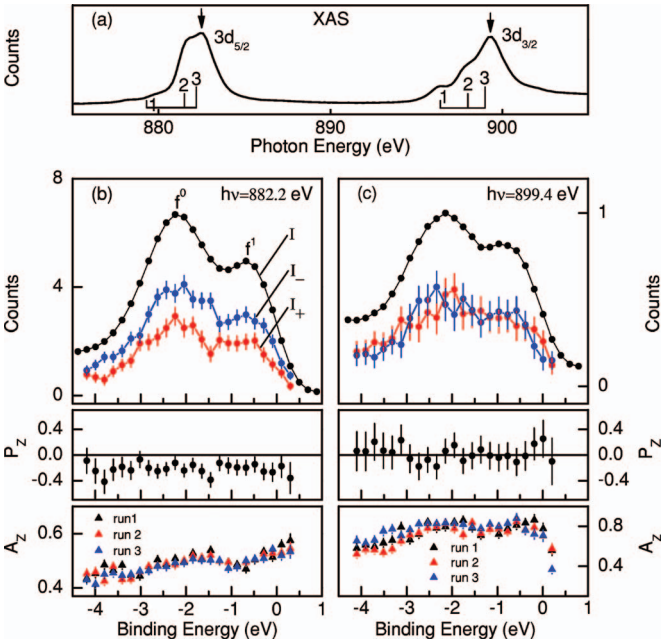

FIG. 3. (Color) (a) $3d \rightarrow 4f$ x-ray absorption spectroscopy (XAS) of Ce. Vertical lines with numbers indicate the observed three different multiplet states of the intermediate $3d^9 4f^2$ configuration from Ref. 30. Arrows show the two photon energies used for spin-resolved resonant photoemission measurements given in (b) and (c). (b) and (c) spin-resolved resonant photoemission spectra measured at $3d_{5/2} \rightarrow 4f$ at $h\nu = 882.2$ eV and $3d_{3/2} \rightarrow 4f$ at $h\nu = 899.4$ eV, respectively. I is the spin integrated total intensity, and I_+ (red) and I_- (blue) are the two spin separated partial intensities. For comparison, the total intensity of $3d_{5/2} \rightarrow 4f$ is normalized by that of $3d_{3/2} \rightarrow 4f$ at the position of f^0. The middle and the bottom panels of (b) and (c) represent electron spin polarization P_Z determined by Eq. (3) and instrumental asymmetries A_Z determined by Eq. (4) for the three independent runs, respectively.

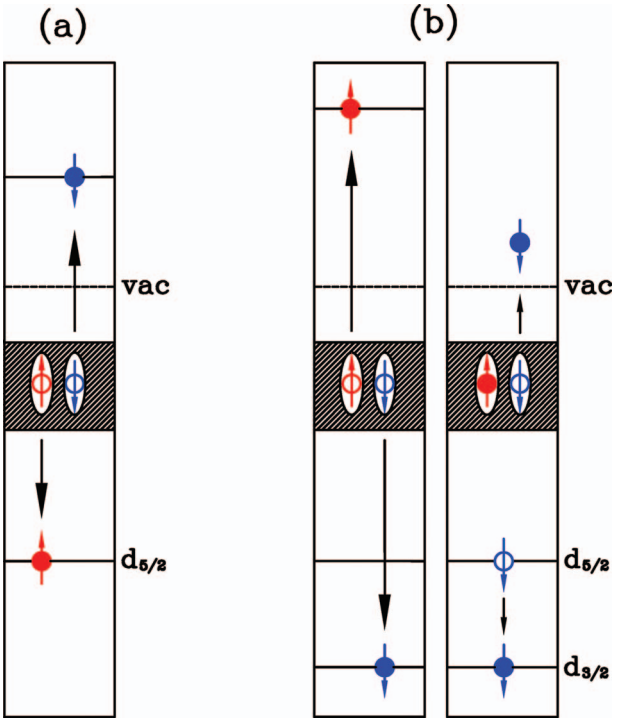

FIG. 4. (Color) (a) A sketch for a singlet coupling in a decay of spin-polarized $3d_{5/2}$ core hole. (b) A sketch for a singlet coupling in a decay of spin-polarized $3d_{3/2}$ core hole (left panel), with an additional Coster-Kronig transition (right panel). Here, the spin-conserving Coster-Kronig process is assumed (Ref. 11). The energy difference is not to scale in (a) and (b).

ure 2 illustrates a scheme of optical spin orientation in an atom for the $d \rightarrow f$ transition with σ^+. The positive and negative numbers in the rectangles represent the angle integrated spin polarizations for given m_j using the Clebsch-Gordan coefficients. The arrows indicate the allowed transitions between the initial and final states via relativistic dipole selection rules for σ^+ with the transition probabilities calculated using the spherical harmonics with the assumption of identical radial parts of the $d_{5/2}$- and $d_{3/2}$-wave functions in the initial states and of the $f_{7/2}$- and $f_{5/2}$-wave functions in the final states. Because the spin polarization of the final states lead to spin-resolved photoemission if their energy lie above the vacuum level, the spin polarization of photoelectrons can be calculated using the following expression:

$$P = \frac{\sum_{i=-J}^{J} a_i s_i}{\sum_{i=-J}^{J} a_i}. \tag{5}$$

Here, a_i are the transition probabilities and s_i the spin polarizations of the final states. Using Eq. (5) and Fig. 2, the transitions $d_{5/2} \rightarrow f(f_{7/2}+f_{5/2})$ and $d_{3/2} \rightarrow f_{5/2}$ result in the spin polarizations of +60% and −50%, respectively. It should be noted that the $d_{5/2} \rightarrow f_{5/2}$ transition gives a negative spin polarization, but it has 20 times weaker transition probability than that of the $d_{5/2} \rightarrow f_{7/2}$. Therefore, $d_{5/2} \rightarrow f$ $(f_{7/2}+f_{5/2})$ transition gives a net positive spin polarization of photoelectrons.

We notice that there is a poor agreement between the measured spin polarization of +20% and the calculated one of +60% for $d_{5/2} \rightarrow f(f_{7/2}+f_{5/2})$ transition. For this discrepancy, we should note the following two points. Firstly, the measured partial intensities I_+ and I_- include the unpolarized background. A proper subtraction of the background from the partial intensities I_+ and I_- results in a spin polarization of approximately +44% in the peak A which is much closer to +60%. Secondly, the atomic model used in Fig. 2 oversimplifies the real system. For example, the spin polarization of $3d_{5/2} \rightarrow 4f$ transition depends on the photon energy through the radial parts of the matrix elements,[7,9] but the dependency is not included in the atomic model. In any case, even though the atomic model given in Fig. 2 describes the system under study qualitatively only, it is extremely useful because it presents a simple picture how photoelectrons are spin polarized without any complicated calculations.

Another aspect of the spin-resolved direct photoemission of core levels is that it provides an important illustration of the generation of a spin polarized core hole, which is the

basic source for nonzero spin polarization in the resonant photoemission experiment. In the direct photoemission of core levels, the circularly polarized light produces spin-polarized photoelectrons due to the relativistic dipole selection rules. This means, because photoelectrons are spin polarized, they should leave behind spin-polarized core holes in the initial states. Based on Fig. 2, due to the different transition probabilities for the different m_j, the $3d_{5/2} \rightarrow 4f$ transitions with σ^+ gives rise to an anisotropic excitation in the m_j of $3d_{5/2}$, generating a net +47% spin-polarized core hole in the $3d_{5/2}$ state. Here, Eq. (5) has been used by substituting s_i with the spin polarizations of m_j of a $3d_{5/2}$ state. The meaning of spin-polarized core hole is that the sum of the m_j of $3d_{5/2}$ core holes is not equal to zero.[10] In the same way, the $3d_{3/2} \rightarrow 4f$ transitions create a −30% spin polarized core hole in the $3d_{3/2}$-state. These spin-polarized core holes will decay by the spin-dependent CVV Auger processes, contributing to the resonant photoemission through the indirect channel.

Now, let us consider the resonant photoemission itself. Figures 3(b) and 3(c) present spin-resolved resonant photoemission measured at the $3d_{5/2} \rightarrow 4f$ transition at $h\nu = 882.2$ eV and the $3d_{3/2} \rightarrow 4f$ transition at $h\nu = 899.4$ eV. At the $3d_{5/2} \rightarrow 4f$ resonance, the partial intensity I_- is dominant over the two peaks labeled as f^0 and f^1,[21,48] with a monotonic −20% spin polarization. This observation and the impact of the negative spin polarization at the $3d_{5/2} \rightarrow 4f$ resonance is the main message of this paper. As shown in Fig. 4(a), we propose a simplified physical explanation for the measured spin polarization. The positively spin-polarized core holes in the $3d_{5/2}$ state decay obey the selection rule for the CVV Auger-like process; the two valence f electrons coupled in a singlet participate in the decay process, result in a −20% spin polarization. In principal, the spin polarization from the direct photoemission and the indirect CVV part can both contribute to the spin polarization measured at resonance. As shown below, however, the contribution from the direct photoemission can be suppressed because uncrystallized Ce samples were used instead of a single crystal in the measurements. In photoemission from nonmagnetic valence bands, a significant nonzero spin polarization can be expected only at points and along lines of high symmetry in the Brillouin zone because there are spatially degenerated bands and spin-orbit interaction splits the bands. These bands modified by the spin-orbit interaction and circularly polarized light are the necessary conditions for nonzero spin polarization. However, at the general points of the Brillouin zone, where there are no spatially degenerated bands to be modified by spin-orbit interaction, photoelectrons are unpolarized giving equal amounts of "up" and "down" spins.[1,49] An example is the spin-resolved valence band photoemission from Ge; electrons emitted from a Ge(001) single crystal using circularly polarized light are highly spin polarized while electrons emitted from amorphous Ge film at the same photon energy are unpolarized.[1] Since we used uncrystallized Ce samples, which have no well defined points and lines of symmetry, we expect that there is no contribution in the measured spin polarization from the direct photoemission. Therefore, we conclude that the −20% spin polarization measured in the resonant spectra results from correlations in the spins between the polarized core holes and the outgoing Auger electrons, mediated by two valence f electrons coupled in a singlet.

The appearance of the two peaks f^0 and f^1 is characteristic of the highly localized nature of $4f$ electrons assumed to be similarly localized to core electrons. A hole created in the $4f$ state by photoemission acts as an additional attractive potential for the other electrons in the system, generating complicated final states as f^0 and f^1 (Ref. 21). The monotonic spin polarization measured over the two peaks f^0 and f^1 indicates that the f^0 and f^1 states are resonated with the identical spin structure. It should be noted that the two peaks f^0 and f^1 are also assigned as the lower Hubbard band and the quasiparticle peak, respectively.[40,50–52]

In the same vein, a positive spin polarization is expected at the $3d_{3/2} \rightarrow 4f$ resonance because of a negatively spin-polarized core hole in the $3d_{3/2}$ state. As shown in Fig. 3(c), however, no spin polarization is observed at the $3d_{3/2} \rightarrow 4f$ resonance, within the statistics. In addition, a direct comparison of the total intensities of the $3d_{5/2} \rightarrow 4f$ and the $3d_{3/2} \rightarrow 4f$ transitions at the position of f^0, indicates that there is an approximately 6.5 times reduction in the intensity at the $3d_{3/2} \rightarrow 4f$ resonance relative to that at the $3d_{5/2} \rightarrow 4f$ resonance. It appears that the CVV indirect channel of the $3d_{3/2}$ core hole has been quenched by a competitive decay channel, a Coster-Kronig (CK) transition, where the spin-polarized core hole in the $3d_{3/2}$ state is filled by electrons from the $3d_{5/2}$ state, resulting in spin-polarized holes in $3d_{5/2}$ and the production of off-resonance electrons with lower kinetic energy. Since the CK transition commonly occurs with 1–3 orders of magnitude greater probability than the usual Auger decay and degrades the spin polarization of the polarized holes in the $3d_{3/2}$(Refs. 10 and 53), the consequence is the substantial decrease of the intensity and the spin polarization at the $3d_{3/2} \rightarrow 4f$ resonance, as shown in Fig. 4(b).

The comparison between the −20% spin polarization measured at the $3d_{5/2} \rightarrow 4f$ resonance and the −47% spin polarization of the $3d_{5/2}$ core holes calculated using the atomic model shows clearly a considerable discrepancy, although we understand that the atomic model explains the measured spin polarization qualitatively only. Even though the discrepancy does not prevent us from understanding the spin-spin coupling basically, some possible reasons for the discrepancy are addressed in the following.

(i) Triplet coupled two electrons may participate in the resonant process. Although the singlet coupling is favored, triplet coupling may have some influence.

(ii) A recent publication on Ce compounds[54] indicated that there are incoherent Auger transitions between different multiplet states of a $3d^9 4f^2$ configuration in the resonant process. Assuming the incoherent Auger electrons are unpolarized, they are overlapped with the main resonant signal as an unpolarized background, thereby lowering the spin polarization.[55]

(iii) Because the matrix element of the Auger process is described by the integration of the initial state (two $4f$ states

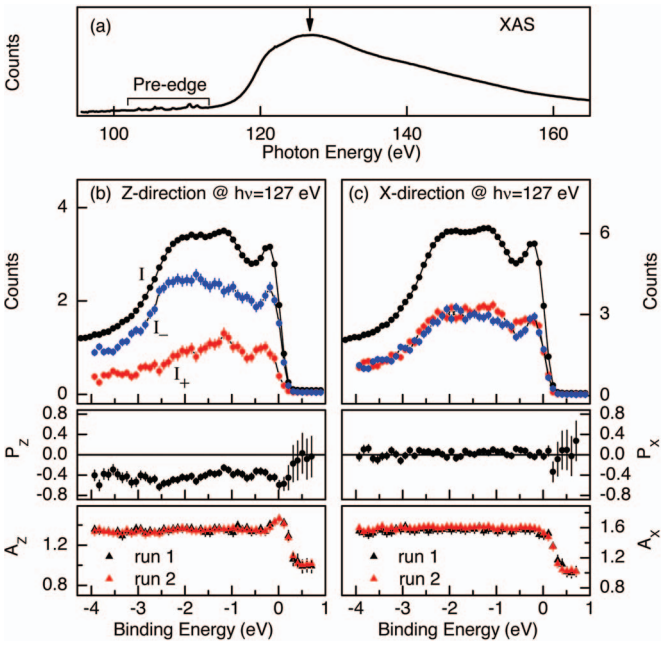

FIG. 5. (Color) (a) $4d \rightarrow 4f$ x-ray absorption spectroscopy (XAS) of Ce. The arrow shows the photon energy used for the spin-resolved resonant photoemission measurement given in (b) and (c). (b) Spin-resolved resonant photoemission spectra measured at $4d \rightarrow 4f$ resonance along the *Z*-direction (parallel to the photon propagation direction) at $h\nu = 127$ eV. *I* is the spin integrated total intensity, and I_+ (red) and I_- (blue) are the two spin separated partial intensities. The middle and the bottom panels of (b) represent the electron spin polarization P_Z determined by Eq. (3) and instrumental asymmetries A_Z determined by Eq. (4) for the two independent runs, respectively. (c) Spin-resolved resonant photoemission spectra measured at $4d \rightarrow 4f$ resonance along the *X*-direction (perpendicular to the photon propagation direction) at $h\nu = 127$ eV. The middle and the bottom panels of (c) represent electron spin polarization P_X determined by Eq. (3) and instrumental asymmetries A_X determined by Eq. (4) for the two independent runs, respectively.

representing two *f* electrons) and the final state ($3d$ core state and a continuum wave function representing the Auger electron), the overlap of the wave functions of the initial and the final states may play a role for an effective correlation between electrons involved in the Auger process. A complete overlap between those wave functions could result in a large exchange interaction, causing a complete spin correlation of electrons involved in the Auger process, while a relatively small overlap could result in a small correlation, reducing the spin polarization of the Auger electron. In fact, the overlap between the $4d$ and $4f$ wave functions is stronger than that between the $3d$ and $4f$ wave functions.[30] In support of the above argument, spin-resolved resonance spectra of the $4d \rightarrow 4f$ resonance at $h\nu = 127$ eV using circularly polarized light are shown in Fig. 5. The measurements with the uncrystallized Ce sample were performed at the beamline 4 at the Advanced Light Source, Lawrence Berkeley National Laboratory and a detailed experimental setup is described elsewhere.[56] The basic pressures were in the low 10^{-11} torr range, during both the measurements and the evaporation. At the $4d$ threshold, both the pre-edge structure and a broad giant resonance, which are a manifestation of strong Coulomb and exchange interaction between $4d$ and $4f$,[20,32] are observed in the x-ray absorption spectroscopy as shown in Fig. 5(a). Figures 5(b) and 5(c) illustrate spin-resolved resonant photoemission spectra measured at $h\nu = 127$ eV along the *Z* direction aligned with the photon propagation direction and along the *X*-direction perpendicular to that, respectively. It is clear that because the incoming circularly polarized light creates spin-polarized core holes aligned with the photon propagation direction, there is no physical driving force for nonzero spin polarization along the *X* direction. As shown in Fig. 5(c), P_X is equal to zero within the statistic error bars. The physical origin of the measured spin polarization P_Z at the $4d \rightarrow 4f$ resonance is also the spin-polarized core hole at the $4d_{5/2}$ created by circularly polarized light. The spin-orbit coupling of $4d_{5/2}$ and $4d_{3/2}$ is small. However, the core holes generated at the $4d_{3/2}$ edge decay via the CK transition into the $4d_{5/2}$ core holes. Therefore, the $4d_{3/2}$ core holes do not influence the spin polarization measured at the $4d \rightarrow 4f$ resonance.[10] As shown in Fig. 5(b), spin polarization P_Z measured over the $4d \rightarrow 4f$ resonance is approximately -43%, which agrees almost quantitatively with the -47% predicted by the atomic model. Thus an "overlap" scenario may explain why the spin polarization measured at the $3d_{5/2} \rightarrow 4f$ resonance is low. A detailed analysis of spin-resolved resonance spectra at the $4d \rightarrow 4f$ resonance will be covered in a future work.

More evidently, high resolution photoemission experiments demonstrated that while the $3d \rightarrow 4f$ resonance probes the bulk $4f$ states, the $4d \rightarrow 4f$ resonance probes mainly the surface $4f$ states which are much more localized and atomiclike than the bulk $4f$ states.[57,58] Due to the strongly localized (atomic) character of the surface $4f$ states, the $4d \rightarrow 4f$ resonance may produce a higher spin polarization than that of the $3d \rightarrow 4f$ resonance.

In conclusion, spin-dependent resonant photoemission using circularly polarized light has been applied to explore the spin-spin coupling between two *f* electrons of strongly correlated nonmagnetic Ce. Positively and negatively spin polarized core holes are created at spin-orbit split $3d_{5/2}$ and $3d_{3/2}$ states, respectively, by direct photoemission using circularly polarized light. At the $3d_{5/2} \rightarrow 4f$ resonance, the measured monotonic negative spin polarization reveals a dominant singlet coupling between two $4f$ electrons participating in the resonant process. Because the Auger process is driven by a Coulomb interaction, the singlet coupling is favored because it allows the two electrons to be in greater proximity than the triplet coupling. At the $3d_{3/2} \rightarrow 4f$ resonance the spin polarization is quenched via an additional CK process. The negative spin polarization measured at the $4d \rightarrow 4f$ resonance also supports the singlet coupling. Based on the Ce results, we would like to suggest that spin-dependent resonant photoemission may provide an excellent way to probe the *f*-electron correlations in rare earth. Finally, from the experimental point of view, theoretical calculations for spin-resolved resonant photoemission are highly desirable to understand the electron correlations quantitatively.

This work was performed under the auspices of the U. S. Department of Energy by the University of California, Lawrence Livermore National Laboratory under Contract

No. W-7405-Eng-48. The experiments were performed at the beamline 4-ID-C at the APS, all of which were constructed and funded by the Office of Basic Energy Science at the U.S. Department of Energy.

*Corresponding author. Electronic address: YU21@LLNL.GOV

[1] F. Meier and D. Pescia, *Optical Orientation*, edited by F. Meier and B. P. Zakharchenya (Elsevier, Amsterdam, 1984).
[2] M. Wöhlecke and G. Borstel, *Optical Orientation*, edited by F. Meier and B. P. Zakharchenya (Elsevier, Amsterdam, 1984).
[3] A. Eyers, F. Schäfers, G. Schönhense, U. Heinzmann, H. P. Oepen, K. Hünlich, J. Kirschner, and G. Borstel, Phys. Rev. Lett. **52**, 1559 (1984).
[4] B. Kessler, A. Eyers, K. Horn, N. Müller, B. Schmiedeskamp, G. Schönhense, and U. Heinzmann, Phys. Rev. Lett. **59**, 331 (1987).
[5] S.-W. Yu, N. Müller, U. Heinzmann, C. Pettenkofer, A. Klein, and P. Blaha, Phys. Rev. B **69**, 045320 (2004).
[6] U. Heinzmann, Phys. Scr., T **17**, 77 (1987).
[7] U. Fano, Phys. Rev. **178**, 131 (1969); Phys. Rev. **184**, 250 (1969).
[8] U. Heinzmann, J. Kessler, and J. Lorenz, Phys. Rev. Lett. **25**, 1325 (1970).
[9] K. Starke, A. P. Kaduwela, Y. Liu, P. D. Johnson, M. A. Van Hove, C. S. Fadley, V. Chakarian, E. E. Chaban, G. Meigs, and C. T. Chen, Phys. Rev. B **53**, R10544 (1996).
[10] P. Stoppmanns, Ph.D. thesis, Universität Bielefeld, Germany, 1995.
[11] R. David, M. Scheuer, P. Stoppmanns, S.-W. Yu, N. Müller, and U. Heinzmann, J. Electron Spectrosc. Relat. Phenom. **93**, 153 (1998).
[12] N. Müller, T. Lischke, M. R. Weiss, and U. Heinzmann, J. Electron Spectrosc. Relat. Phenom. **114-116**, 777 (2001).
[13] G. Snell, B. Langer, M. Drescher, N. Müller, B. Zimmermann, U. Hergenhahn, J. Viefhaus, U. Heinzmann, and U. Becker, Phys. Rev. Lett. **82**, 2480 (1999).
[14] T. Kachel, R. Rochow, W. Gudat, R. Jungblut, O. Rader, and C. Carbone, Phys. Rev. B **45**, 7267 (1992).
[15] L. H. Tjeng, B. Sinkovic, N. B. Brookes, J. B. Goedkoop, R. Hesper, E. Pellegrin, F. M. F. de Groot, S. Altieri, S. L. Hulbert, E. Shekel, and G. A. Sawatzky, Phys. Rev. Lett. **78**, 1126 (1997).
[16] N. B. Brookes, G. Ghiringhelli, O. Tjernberg, L. H. Tjeng, T. Mizokawa, T. W. Li, and A. A. Menovsky, Phys. Rev. Lett. **87**, 237003 (2001).
[17] P. G. Steeneken, L. H. Tjeng, I. Elfimov, G. A. Sawatzky, G. Ghiringhelli, N. B. Brookes, and D.-J. Huang, Phys. Rev. Lett. **88**, 047201 (2002).
[18] S. Suga, A. Kimura, T. Matsushita, A. Sekiyama, S. Imada, K. Mamiya, A. Fujimori, H. Takahashi, and N. Mori, Phys. Rev. B **60**, 5049 (1999).
[19] T. A. Carlson, *Photoelectron and Auger Spectroscopy* (Plenum Press, New York, 1975).
[20] K. T. Moore, B. W. Chung, S. A. Morton, A. J. Schwartz, J. G. Tobin, S. Lazar, F. D. Tichelaar, H. W. Zandbergen, P. Söderlind, and G. van der Laan, Phys. Rev. B **69**, 193104 (2004).
[21] S. Hüfner, *Photoelectron Spectroscopy*, 3rd ed. (Springer-Verlag, Berlin, 2003).
[22] R. C. Albers, Nature (London) **410**, 759 (2001).
[23] S. Y. Savrasov, G. Kotliar, and E. Abrahams, Nature (London) **410**, 793 (2001).
[24] J. G. Tobin, K. T. Moore, B. W. Chung, M. A. Wall, A. J. Schwartz, G. van der Laan, and A. L. Kutepov, Phys. Rev. B **72**, 085109 (2005).
[25] J. W. Freeland, J. C. Lang, G. Srajer, R. Winarski, D. Shu, and D. M. Mills, Rev. Sci. Instrum. **73**, 1408 (2002).
[26] M. Hochstrasser, J. G. Tobin, E. Rotenberg, and S. D. Kevan, Phys. Rev. Lett. **89**, 216802 (2002).
[27] S. A. Morton, G. D. Waddill, S. Kim, Ivan K. Schuller, S. A. Chambers, and J. G. Tobin, Surf. Sci. Lett. **513**, L451 (2002).
[28] J. G. Tobin *et al.*, in *Application of Synchrotron Radiation Techniques to Materials Science IV*, edited by S. M. Mini *et al.*, MRS Symposia Proceedings No. 524 (Materials Research Society, Pittsburgh, 1998), p. 185.
[29] E. Weschke, A. Höhr, G. Kaindl, S. L. Molodtsov, S. Danzenbächer, M. Richter, and C. Laubschat, Phys. Rev. B **58**, 3682 (1998).
[30] C. Bonnelle, R. C. Karnatak, and J. Sugar, Phys. Rev. A **9**, 1920 (1974).
[31] S. Pagliara, L. Sangaletti, C. Cepek, F. Bondino, R. Larciprete, and A. Goldoni, Phys. Rev. B **70**, 035420 (2004).
[32] S. R. Mishra, *et al.* , Phys. Rev. Lett. **81**, 1306 (1998).
[33] J. Kessler, *Polarized Electrons*, 2nd ed. (Springer-Verlag, Berlin, 1985).
[34] G. Crecelius, G. K. Wertheim, and D. N. E. Buchanan, Phys. Rev. B **18**, 6519 (1978).
[35] J. M. Esteva, R. C. Karnatak, J. C. Fuggle, and G. A. Sawatzky, Phys. Rev. Lett. **50**, 910 (1983).
[36] A. Kotani and Y. Toyozawa, J. Phys. Soc. Jpn. **37**, 912 (1974).
[37] F. U. Hillebrecht and J. C. Fuggle, Phys. Rev. B **25**, 3550 (1982).
[38] O. Gunnarsson and K. Schönhammer, Phys. Rev. Lett. **50**, 604 (1983).
[39] O. Gunnarsson and K. Schönhammer, Phys. Rev. B **28**, 4315 (1983).
[40] G. Kotliar and D. Vollhardt, Phys. Today **57**(3), 53 (March 2004).
[41] I. Adawi, Phys. Rev. A **134**, 788 (1964).
[42] J. B. Pendry, Surf. Sci. **57**, 679 (1976).
[43] W. L. Schaich, in *Photoemission in Solids I*, edited by M. Cardona and L. Ley (Springer-Verlag, Berlin, 1978).
[44] C. N. Berglung and W. E. Spicer, Phys. Rev. **136**, 1030 (1964).
[45] J. Kirschner, R. Feder, and J. F. Wendelken, Phys. Rev. Lett. **47**, 614 (1981).
[46] G. D. Waddill, J. G. Tobin, X. Guo, and S. Y. Tong, Phys. Rev. B **50**, 6774 (1994).
[47] J. G. Tobin and F. O. Schumann, Surf. Sci. **478**, 211 (2001).
[48] E. Weschke, C. Laubschat, T. Simmons, M. Domke, O. Strebel, and G. Kaindl, Phys. Rev. B **44**, 8304 (1991).
[49] R. J. Elliott, Phys. Rev. **96**, 280 (1954).
[50] M. B. Zolfl, I. A. Nekrasov, Th. Pruschke, V. I. Anisimov, and J. Keller, Phys. Rev. Lett. **87**, 276403 (2001).
[51] K. Held, A. K. McMahan, and R. T. Scalettar, Phys. Rev. Lett.

87, 276404 (2001).
[52] K. Haule, V. Oudovenko, S. Y. Savrasov, and G. Kotliar, Phys. Rev. Lett. **94**, 036401 (2005).
[53] R. G. Oswald and T. A. Callcott, Phys. Rev. B **4**, 4122 (1971).
[54] E. J. Cho, R. J. Jung, B. H. Choi, S. J. Oh, T. Iwasaki, A. Sekiyama, S. Imada, S. Suga, T. Muro, J. G. Park, and Y. S. Kwon, Phys. Rev. B **67**, 155107 (2003).
[55] O. Tjernberg, M. Finazzi, L. Duo, G. Ghiringhelli, P. Ohresser, and N. B. Brookes, Physica B **281**, 723 (2000).
[56] J. G. Tobin, S. A. Morton, B. W. Chung, S. W. Yu, and G. D. Waddill (unpublished).
[57] A. Sekiyama, T. Iwasaki, K. Matsuda, Y. Saitoh, Y. Onuki, and S. Suga, Nature (London) **403**, 396 (2000).
[58] A. Sekiyama, K. Kadono, K. Matsuda, T. Iwasaki, S. Ueda, S. Imada, S. Suga, R. Settai, H. Azuma, Y. Onuki, and Y. Saitoh, J. Phys. Soc. Jpn. **69**, 2771 (2000).